Vapor-liquid coexistence of the Stockmayer fluid in nonuniform external fields

Sela Samin and Yoav Tsori*
Department of Chemical Engineering and The Ilse Katz Institute for Nanoscale Science and Technology, Ben-Gurion University of the Negev, 84105 Beer-Sheva, Israel

Christian Holm
Institut für Computerphysik, Universität Stuttgart, Allmandring 3, D-70569 Stuttgart,Germany
(Received 28 February 2013; published 22 May 2013)

We investigate the structure and phase behavior of the Stockmayer fluid in the presence of nonuniform electric fields using molecular simulation. We find that an initially homogeneous vapor phase undergoes a local phase separation in a nonuniform field due to the combined effect of the field gradient and the fluid vapor-liquid equilibrium. This results in a high-density fluid condensing in the strong field region. The system polarization exhibits a strong field dependence due to the fluid condensation.

DOI: 10.1103/PhysRevE.87.052128 PACS number(s): 61.20.Ja, 64.70.F−, 68.03.−g

I. INTRODUCTION

The application of external fields for manipulation of the structure and phase behavior of dipolar fluids has attracted growing interest in recent years [1,2]. Typically, both theoretical and experimental studies consider uniform applied fields. However, in complex systems, such as microfluidic devices, field gradients occur naturally. Motivated by experimental work on the demixing of binary mixtures in field gradients [3], we have previously studied theoretically the application of nonuniform electric fields to pure fluids [4] and simple mixtures [5,6]. Another experimental realization of the ability of field gradients to promote phase transitions is the field-induced crystallization of colloidal suspensions promoted by dielectrophoretic forces [7–9].

In particular, we examined the effect of nonuniform fields on the vapor-liquid coexistence [4] by combining the simple van der Waals mean-field theory with Onsager's theory of dielectrics to investigate polar and nonpolar fluids. Our main finding was that above a critical field, in situations where the fluid is unperturbed by a uniform field, a nucleation of a gas bubble from the liquid phase or a liquid droplet from the vapor phase is induced by a nonuniform field. This phase separation transition is promoted by the dielectrophoretic force which favors a higher permittivity (density) fluid in the region of strong field. The resulting modification in the fluid phase diagram is considerably larger compared to uniform fields.

A system which can be considered as an idealized manifestation of nonuniform fields is a grand canonical ensemble where a uniform field, $\boldsymbol{E} = \text{const.}$, is applied within the system volume but not in the material reservoir, where $\boldsymbol{E} = 0$. An example is a slit pore in equilibrium with a bulk fluid. The field effect in this type of system has been studied for one component fluids [10,11] where it was found to gradually increase the fluid density within the pore moderately. A stronger field effect was found by Brunet *et al.* [12,13] who studied mixtures. They observed that if the mixture has a demixing instability and one of the components is dipolar, the coupling to the external field leads to a pore filling transition which allows a sensitive control of the pore composition. However, in real systems there exists an interfacial region at the pore edges where the field is nonuniform.

The goal of this paper is to study the structure of a dipolar vapor confined in a slit pore and exposed to nonuniform electric fields in the canonical ensemble via molecular simulation. We compare our results with mean field theory and discuss the consequences of the full description of the vapor-liquid interface in finite systems. The paper is organized as follows. Section II discusses the simulation methods and model system. Section III A compares results for the fluid in a uniform field with previous studies. The results for a nonuniform field are compiled in Sec. III B. Conclusions are given in Sec. IV.

II. SIMULATION METHODS

We consider N spherical dipolar particles with a diameter σ and a permanent dipole moment $\boldsymbol{\mu}$. The particles interact via the Stockmayer pair potential:

$$U_{ij} = 4\epsilon\left[\left(\frac{\sigma}{|\boldsymbol{r}_{ij}|}\right)^{12} - \left(\frac{\sigma}{|\boldsymbol{r}_{ij}|}\right)^{6}\right] + \frac{1}{4\pi\varepsilon_0}\left(\frac{\boldsymbol{\mu}_i\cdot\boldsymbol{\mu}_j}{|\boldsymbol{r}_{ij}|^3} - \frac{3(\boldsymbol{\mu}_i\cdot\boldsymbol{r}_{ij})(\boldsymbol{\mu}_j\cdot\boldsymbol{r}_{ij})}{|\boldsymbol{r}_{ij}|^5}\right), \quad (1)$$

where $\boldsymbol{r}_{ij} = \boldsymbol{r}_i - \boldsymbol{r}_j$ stands for the displacement vector of particles i and j, ϵ denotes the Lennard-Jones (LJ) interaction parameter, and ε_0 is the vacuum permittivity. In the following we use reduced units; length: $r^* = r/\sigma$, temperature: $T^* = k_BT/\epsilon$, density: $\rho^* = \rho\sigma^3$, dipole moment: $\mu^* = \mu/\sqrt{4\pi\varepsilon_0\epsilon\sigma^3}$, and external field: $E^* = E\sqrt{4\pi\varepsilon_0\epsilon\sigma^3}$. Here, k_B is the Boltzmann constant and we take $\sigma = \epsilon = 4\pi\varepsilon_0 = 1$. For brevity we omit the asterisk superscript henceforth.

The phase diagram of bulk and confined Stockmayer fluids in a uniform field was determined using a Gibbs Ensemble–Hybrid Monte Carlo scheme (GE-HMC). The classical Gibbs Ensemble Monte Carlo (GEMC) simulation [14] offers a simple method to determine the vapor-liquid equilibrium densities and pressures with a single simulation run. This is achieved by equating the chemical potentials and pressures of two simulation boxes using appropriate Monte Carlo particle

*tsori@bgu.ac.il

 ©2013 American Physical Society

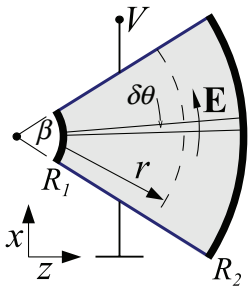

FIG. 1. (Color online) The model capacitor: a wedge made of two flat electrodes with a potential difference V across them and an angle β between them. R_1 (R_2) is the distance of the inner (outer) insulating wall from the imaginary meeting point of the electrodes (thick lines). r is the radial distance from the inner wall. The resulting electric field $\mathbf{E}$ is along the $\hat{\theta}$ direction. In the simulations we approximate a small angular segment $\delta\theta$ as a slit.

and volume exchange moves, respectively [15]. The third type of moves performed are particle translations, rotations, and other conformational changes of single particles within the two boxes. In the GE-HMC variation, single particle moves are replaced by a collective Hybrid Monte Carlo (HMC) move [16,17]. A single HMC cycle consists of three steps: first, particles of the current configuration, o, are assigned new momenta and angular velocities by sampling a Gaussian distribution corresponding to the desired temperature. Second, the new configuration, n, is generated from a short MD trajectory in the microcanonial ensemble. Lastly, the new configuration is accepted or rejected according to the Metropolis criterion:

$$\min(1, \exp(-\Delta H/T)), \tag{2}$$

where $\Delta H = H(n) - H(o)$ is the resulting change in the system Hamiltonian. Detailed balance is satisfied if the integration algorithm used for the MD trajectory is time reversible and area preserving [17], which is fulfilled by a simple velocity-Verlet integrator. All MD trajectories were produced with the ESPResSo package [18]. The collective HMC moves allow to efficiently sample the high density liquid phase and complex molecular configurations [19].

GE-HMC simulation cycles were conducted with 512 Stockmayer particles. The total simulation consisted of 10^4 cycles and observable sampling was done after 2500 equilibration cycles. A single cycle was composed of 100 MC moves where the probability of the move type was as follows: 0.8 for a particle exchange move, 0.15 for a HMC move, and 0.05 for a volume exchange move. The number of time steps in a HMC move was 10. Both the time step and the attempted volume change were adjusted during equilibration such that approximately 50% of the moves were accepted.

Simulations in a nonuniform field and in the canonical ensemble where performed in a simplified model system, see Fig. 1. Consider the fluid confined in a closed wedge capacitor at constant temperature. The capacitor is made up from two flat electrodes with a potential difference V across them and an angle β between them. In this geometry the field in the azimuthal direction is perpendicular to the field gradient in the radial direction. This simplifies the solution of Gauss' law since it implies $\nabla\varepsilon \cdot \mathbf{E} = 0$ [4]. The resulting electric field is

$$\mathbf{E}(r) = \frac{V/\beta}{R_1 + r}\hat{\theta}, \tag{3}$$

where R_1 is the radius of the inner capacitor wall, $R_1 + r$ the radial distance from the imaginary meeting point of the electrodes and θ is the azimuthal angle. We focus on a small angular section $\delta\theta$ far from the electrodes of the capacitor and therefore rewrite Eq. (3) in terms of Cartesian coordinates:

$$\mathbf{E}(z) = \frac{E_0}{1 + A_0 z}\hat{x}, \tag{4}$$

where $E_0 = V/(\beta R_1)$ is the maximal field at $z = 0$ and $A_0 = 1/R_1$ is a constant characterizing the length scale of the field gradient; for $A_0 = 0$ the field is uniform.

In this paper we study the Stockmayer fluid under the external field given in Eq. (4). The contribution of this field to the potential energy of a single particle is given by

$$U_i^{\text{ext}} = -\boldsymbol{\mu}_i \cdot \boldsymbol{E}_i = -\frac{\mu_{i,x} E_0}{1 + A_0 z_i}, \tag{5}$$

where $\boldsymbol{E}_i$ is the field at the site of particle i which is a function of the particle coordinate z_i. Via the potential energy we derive the additional force and torque on particle i due to the field, i.e.,

$$\boldsymbol{F}_i^{\text{ext}} = -\frac{\mu_{i,x} A_0 E_0}{(1 + A_0 z_i)^2}\hat{z}, \tag{6}$$

$$\boldsymbol{T}_i^{\text{ext}} = \frac{\mu_{i,z} E_0}{1 + A_0 z_i}\hat{y} - \frac{\mu_{i,y} E_0}{1 + A_0 z_i}\hat{z}. \tag{7}$$

Note that the force contribution, Eq. (6), vanishes in the case of a uniform field. Moreover, Eq. (6) indicates that particles are drawn to the strong field region and feel a stronger force when aligned with the field. This may be thought of as the microscopic origin of the dielectrophoretic force.

MD simulations of the Stockmayer fluid in a nonuniform field were performed using the suitably modified ESPResSo package [18]. During the simulation the LJ potential was cut off at $r_c = 3$ and the long range dipolar potential was evaluated using the dipolar P^3M algorithm [20] with metallic boundary conditions.

When a nonuniform field is applied to the fluid its translational invariance in the direction of the field gradient is broken and therefore periodic boundary conditions (PBC) cannot be used in this direction. However, the implementation of the P^3M method requires that we employ PBC in all directions. Therefore, in the simulations we model the capacitor as an infinite slab with the two confining walls placed at $z = 0$ and $z = D < L$, where L is the cubic simulation box length. The unwanted dipolar interactions between slabs replicated along the z direction are corrected using the dipolar layer correction method of Ref. [21]. This allows us to use a small gap of empty space in the simulation box. In order to isolate the field effect, we use for the fluid-wall interaction a purely repulsive LJ potential shifted and cut off at $r_c = 2^{1/6}$ (WCA potential).

Simulations of the dipolar fluid in the slab where initialized from random particle configurations. In the simulations we employ a Langevin thermostat. A time step of $\Delta t = 0.004$ was used in all simulations. The simulations equilibration period varied from 1×10^5–6×10^5 time steps, depending on the

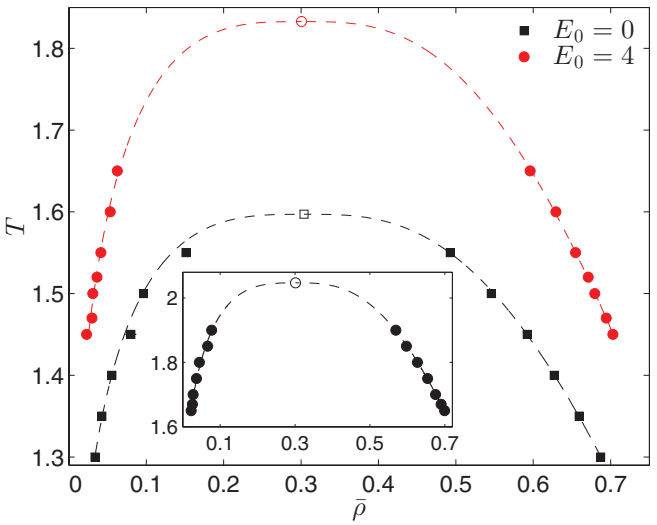

FIG. 2. (Color online) Vapor-liquid coexistence of the bulk Stockmayer fluid with $\mu = 1.5$. Squares: in the absence of an external field. Circles: with a uniform field $E_0 = 4$. Inset: in the absence of an external field for $\mu = 2$. Dashed curves are fits to the law of rectilinear diameters using the Ising exponent $\beta = 0.326$. Critical points are marked by hollow symbols.

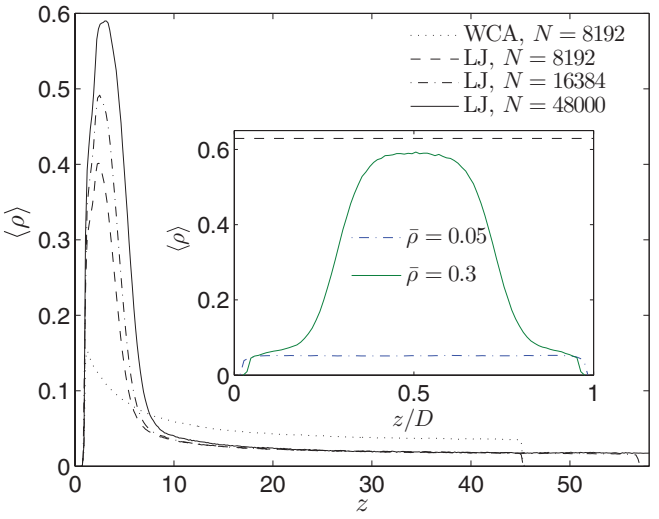

FIG. 3. (Color online) Density profiles $\langle\rho(z)\rangle$ in a nonuniform field for a Stockmayer fluid with an average density $\bar{\rho} = 0.05$ and a temperature $T = 1.6$. For the field we used a magnitude of $E_0 = 4$ in Eq. (4). The dashed curve shows results for $N = 8192$ particles using $A_0 = 0.1$ in Eq. (4). For the dash-dot curve $N = 16384$ and $A_0 = 0.0794$; for the solid curve $N = 48000$ and $A_0 = 0.0555$. Dotted curve: same as the dashed curve but replacing the LJ part of the potential by a WCA potential. Inset: density profiles in a uniform field $\boldsymbol{E} = 4\hat{x}$ at $T = 1.6$. Two average densities, $\bar{\rho} = 0.3$ and 0.05 are presented corresponding to slab widths of $D \approx 25$ and $D \approx 46$, respectively.

field strength. The structural and dielectric properties of the system were then sampled every 200 time steps for at least 4×10^5 time steps. Time averaged quantities sampled are denoted by $\langle\ldots\rangle$.

III. RESULTS AND DISCUSSION

A. Phase behavior of the Stockmayer fluid in a uniform field

We first tested the applicability of our GE-HMC simulation by comparing our results to available data on the Stockmayer fluid with $\mu = 2$. Here, the standard long-range correction is applied to the LJ interaction [15]. The resulting coexistence curve is shown in the inset of Fig. 2. The critical point (T_c, ρ_c) is estimated by fitting the coexistence data to the law of rectilinear diameters: $\rho_l - \rho_g \propto (T_c - T)^\beta$ and $\rho_l + \rho_g = 2\rho_c + C(T_c - T)$, where ρ_l and ρ_g are the liquid and vapor coexistence densities, respectively, $\beta = 0.326$ is the three-dimensional Ising exponent and C is a constant. For $\mu = 2$ we obtain a critical temperature $T_c = 2.05$ and density $\rho_c = 0.301$, in good agreement with the results of van Leeuwen *et al.* [22] ($T_c = 2.06$, $\rho_c = 0.289$) and Kiyohara *et al.* [23] ($T_c = 2.05$, $\rho_c = 0.306$). The small differences in critical parameters are probably due to fact that unlike the works above, the LJ potential in this study is cut off at a fixed radius.

Henceforth, we will focus in this work on the Stockmayer fluid with $\mu = 1.5$. Vapor-liquid coexistence curves for such a bulk Stockmayer fluid with and without an external field are shown in Fig. 2. Here, no long-range correction is applied to the LJ interaction since we intend to compare these results with those obtained in the slab geometry. In the absence of an external field we find $T_c = 1.59$ and $\rho_c = 0.305$. In accord with previous studies, we find when a uniform field is applied the unstable region in the phase plane is increased [24–29]. This is due to the increased dipole-dipole interaction and correlation as the dipoles get aligned by the field [24,29]. In particular, simulations of the Stockmayer fluid in an external field found reasonable agreement with the Landau mean field theory [30] for the field effect on the critical temperature [29]. For $E_0 = 4$ we find that the critical temperature increases to $T_c = 1.83$ and $\rho_c = 0.301$.

The value of $\mu = 1.5$ for the dipole moment was chosen since it is suited for description of both molecular fluids [31] and dipolar colloidal suspension alike [2]. Furthermore, we will from now on set $T = 1.6 < T_c$. Hence, the value of dipolar coupling constant, $\lambda = \mu^2/T$, is $\lambda = 1.41$. This means that the dipolar interaction at a distance σ is comparable to both the thermal and LJ interactions. Note that a λ value close to unity below the critical temperature can only be realized for relatively small values of μ [32].

The effect of confinement on the coexistence curve of the Stockmayer fluid is that of suppression of the unstable region of the phase diagram. Studies conducted so far focused on narrow slabs where this effect is large [33]. The finite-size effects for wider slabs where not studied since they are quite small and also computationally prohibitively expensive.

An estimate of finite-size effects is provided in the inset of Fig. 3, which shows the density profiles, $\langle\rho(z)\rangle$, for $N = 8192$ confined particles at $T = 1.6$ and under an uniform field $\boldsymbol{E} = 4\hat{x}$, parallel to the slab walls. For an average fluid density $\bar{\rho} = 0.3$ (slab width of $D \approx 25$), close to the critical density, the density profile exhibits vapor-liquid coexistence. The dashed horizontal line in the inset corresponds to the liquid phase density $\rho_l = 0.629$ in the absence of confinement. This density is only slightly higher than the average density of $\approx$0.59 for the liquid in the slab and hence the effect of confinement on

the phase coexistence is small. In contrast, slowly expanding the slab such that a fluid average density of $\bar{\rho} = 0.05$ is finally obtained (slab width of $L \approx 46$) results in a homogeneous vapor phase, see the dash-dot curve in the inset of Fig. 3. This is expected since $\bar{\rho} = 0.05$ is smaller than the vapor phase density of the unconfined fluid $\rho_v = 0.053$.

B. The Stockmayer fluid in a nonuniform field

The situation is markedly different when a nonuniform field is applied. The dashed curve in Fig. 3 gives the density profile for $N = 8192$ particles with an average density $\bar{\rho} = 0.05$ under the nonuniform field given by Eq. (4) with $E_0 = 4$ and $A_0 = 0.1$. This profile shows the condensation of a liquid-like layer from the homogeneous vapor phase in the strong field region. The high density layer of width $\approx$2–3σ is followed by a sharp interface and then a distinct vapor phase. The width of the liquid-like layer grows as the fraction of energetically costly interface molecules is reduced in larger systems. This effect is shown in the dash-dot and solid curves in Fig. 3 where we increase the number of particles while keeping the average density the same. Here, since we scale the simulation box to keep the average density constant we also adjust the field in Eq. (4) through A_0 such that $E(z = D)$ is kept constant. In addition, the liquid-like layer density also increases due to the decreased energetic cost of the interface. The increase in the width and density of the liquid-like domain with N and D is a finite size effect which is expected to vanish in the thermodynamic limit $N, D \to \infty$.

We explain this condensation by the fact that the nonuniform field is large only in the vicinity of $z = 0$. Hence, particles are drawn to this region where they gain energetically both by aligning in the stronger field and also from the LJ interaction which compensates for the loss in entropy. The attractive short range part in the interaction is important for the formation of a dense liquid layer. To show this we also performed a simulation where we replace the LJ part of the interaction by the purely repulsive WCA potential. The result for the dipolar WCA fluid is shown in the dotted curve of Fig. 3; clearly, only a moderate increase in the fluid density occurs and it follows the gradual decay of the field.

The Stockmayer potential parameters for water [31] gives $\mu = 1.56$ for the fluid and the field magnitude of $E_0 = 4$ thus corresponds to a maximal local field of 4.1 V/nm. Although the Stockmayer potential is not adequate for water, it is instructive to use it here for the purpose of estimating whether the fields we consider are realistic. Indeed, at least for water confined at the molecular scale field of a few V/nm are not unusual [10]. Nonetheless, this field magnitude is still 5–10 times larger than the fields required to induce condensation in the mean-field treatment [4]. The high field is a consequence of the costly interfacial region in the small system we simulate and is expected to be reduced in the thermodynamic limit.

Figure 4 shows the density profiles obtained as a function of the nonuniform field magnitude, E_0. As E_0 increases the condensation occurs rapidly starting at $E_0 \gtrsim 2.5$ albeit gradually as as our system is finite. The inset of Fig. 4 gives a comparison between the field of Eq. (4) and a nonuniform field of the same functional form and magnitude but *perpendicular* to the slab walls. This type of field is obtained in the zero curvature limit for a capacitor consisting of concentric cylinders [4].

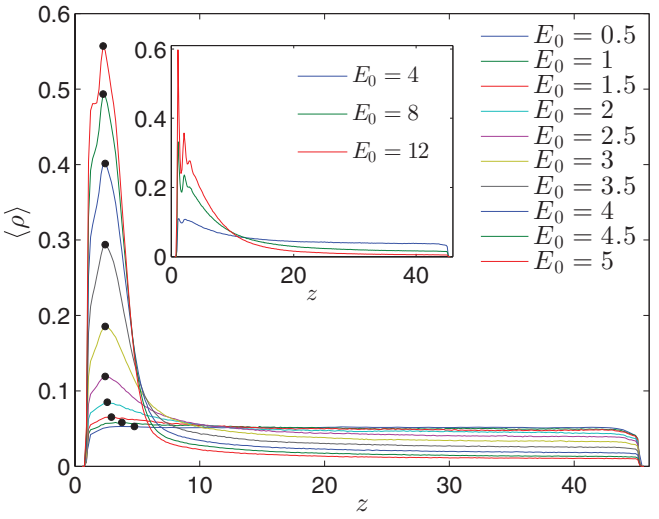

FIG. 4. (Color online) Density profiles $\langle\rho(z)\rangle$ in a nonuniform field of different magnitudes. The fluid maximal density is in the strong field region close to the wall (circle markers) and it increases with the field magnitude. Inset: density profiles for a nonuniform field perpendicular to the slab walls (see text). For all curves $A_0 = 0.1$, the fluid average density is $\bar{\rho} = 0.05$ and the temperature is $T = 1.6$.

It is seen in Fig. 4 that for $E_0 = 4$ the density profile shows a clear condensate in the parallel case. However, for the same value of E_0 in the perpendicular case, $\langle\rho(z)\rangle$ exhibits only a slight increase in the fluid density near the wall. Here, the field introduces a competition between alignment of dipoles parallel to the field, giving rise to the favored head-to-tail configurations, and the creation of an interface parallel to the field which disrupts these configurations [34]. This is in accord with the mean field description in which the typical field required to induce condensation is an order of magnitude larger in the cylindrical capacitor compared to the wedge capacitor [4].

Only upon further increase of E_0 to large values of $E_0 \gtrsim 8$ a significant increase in the density occurs. This is accompanied by large oscillations of the density close to the wall in which the distance between peaks is σ. This is typical when fields perpendicular to the confining walls are applied to a high density dipolar fluid [35]. The oscillatory domain is followed by an interfacial region of width $\approx 10\sigma$, which is large compared to the thin interface of width $\approx 4\sigma$ for parallel fields. Simulation snapshots of a small segment of the system, shown in Fig. 5, illustrate how the orientational order leads to a wider interface in the perpendicular case. We assume that due to the large interfacial energetic penalty in perpendicular fields one must simulate larger systems in order to observe clearly field induced condensation in this case.

In Ref. [6] it was demonstrated that the electric field induced condensation in nonuniform fields is a first order transition. As a result, a discontinuity in the surface density occurs when the field is increased above a critical value. The corresponding quantity in the simulation $\rho_{\max} = \max(\langle\rho(z)\rangle)$ naturally occurs close to the wall where the field is large. In Fig. 6 we plot $\rho_{\max}$ as a function of the field magnitude. We find that $\rho_{\max}(E_0)$ has a

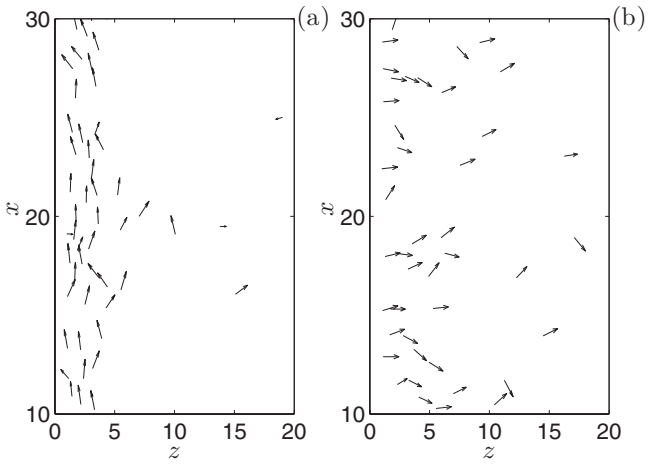

FIG. 5. Snapshots of a thin cross section through the y axis, focusing on the strong field region. Arrows indicate the dipole moment's x and z components scaled by a factor of 2. In (a) the electric field is parallel to the wall and $E_0 = 6$ while in (b) the field is perpendicular to the wall and $E_0 = 12$ is larger. The maximal density near the wall is similar in both panels but the interface is much wider in the perpendicular case due to favored head to tail configurations.

sigmoid like shape, similar to the mean field theory (see Fig. 10 in Ref. [6]). However, since the simulated system is finite $\rho_{\max}(E_0)$ changes continuously. Nonetheless, $\rho_{\max}(E_0)$ grows more rapidly when the number of particles is increased from $N = 8192$ (squares) to $N = 16384$ (circles), suggesting that in the thermodynamic limit a first order transition is realized.

Figure 6 also shows that increasing the average density to $\bar{\rho} = 0.07$ (diamonds) results in a larger condensate density. Although $\bar{\rho} = 0.07$ is inside the binodal for the bulk system, this curve shows that one can utilize the nonuniform field to modify the density profile in a dilute enough finite system, such as a colloidal suspension.

Results for the average dipole moment in the direction of the field $\langle \mu_x(z) \rangle$ are shown in the solid curves of Fig. 7. These

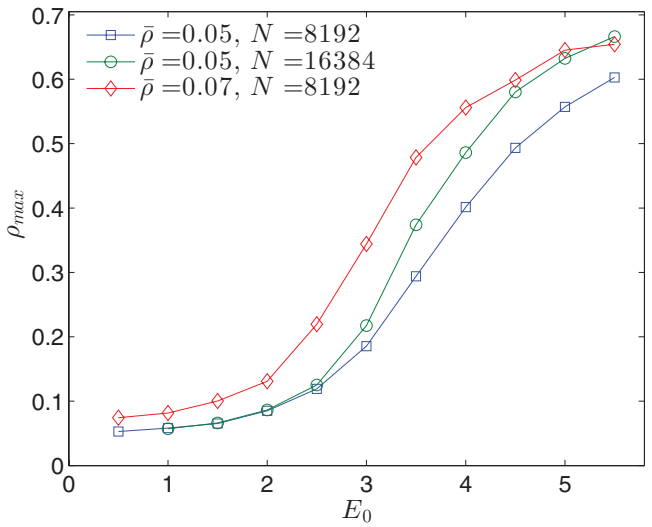

FIG. 6. (Color online) Maximal density as a function of the nonuniform field magnitude. $A_0 = 0.1$ in all curves while the average density or number of particles is varied.

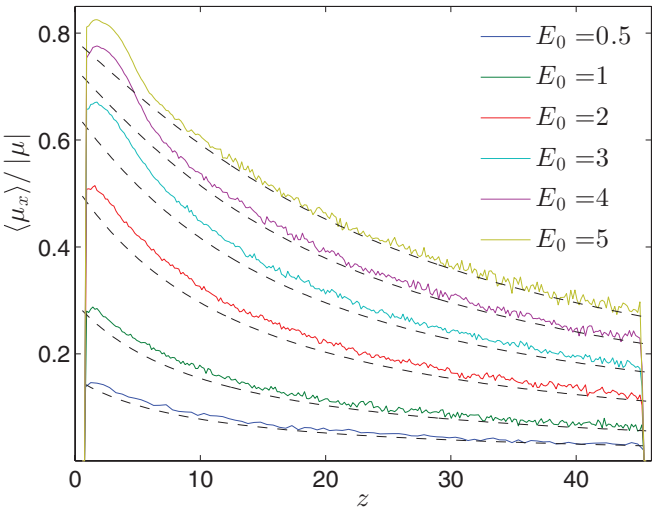

FIG. 7. (Color online) Solid curves: profiles of the scaled x component of the dipole moment $\mu_x/|\mu|$ for several nonuniform field strengths. dashed curves: Debye theory prediction [Eq. (8)].

results are contrasted with the Debye theory [36] for an ideal gas shown in the dash-dot curves of Fig. 7. In the Debye theory,

$$\langle \mu_x(z) \rangle = \mu L(\alpha), \tag{8}$$

where $L(\alpha) = \coth(\alpha) - 1/\alpha$ is the Langevin function and $\alpha = \mu |\boldsymbol{E}(z)| / T$. The simulation results agree with the Debye theory in the dilute vapor region but deviate to higher values in the dense liquid region. The deviation stems from the oversimplified treatment of the dipoles orientation correlation in the Debye theory [37,38] as well as the unaccounted effect of the short range LJ interaction on the orientational correlation.

Further insight to the effect of the nonuniform field is gained by examining the polarization of the system. $\langle \boldsymbol{P} \rangle = \langle \sum_i \boldsymbol{\mu_i} \rangle$. Since in our case $E_z = E_y = 0$, it follows from Eq. (8) that

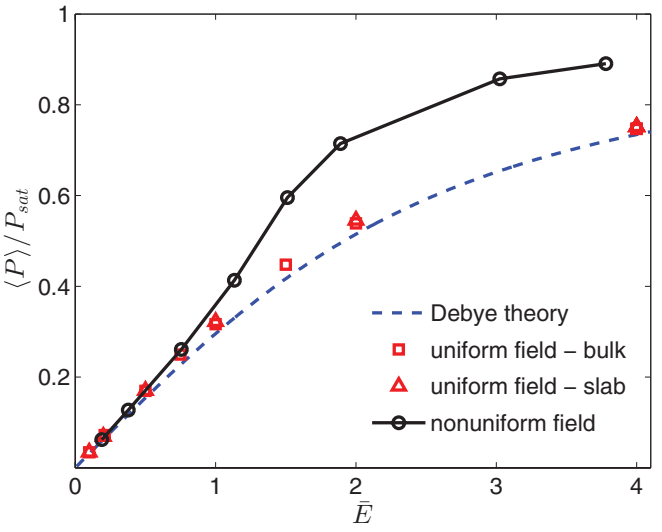

FIG. 8. (Color online) Scaled polarization $\langle P \rangle / P_{\text{sat}}$ as a function of the average field $\bar{E}$. Bulk and slab systems in a uniform field exhibit a Langevin type polarization while in a nonuniform field the polarization is larger starting at $\bar{E} \approx 1$.

for $E_x = \text{const.}$:

$$\langle P \rangle = P_{\text{sat}} L(\alpha), \tag{9}$$

where $P_{\text{sat}} = N\mu$ is the saturation polarization of the system. We compare the polarization for a uniform field in the bulk and in the slab in Fig. 8. Simulation results in both cases are almost identical and agreement with the Debye theory is very good. This indicates that the bulk and slab system's response to a uniform field is essentially the same here because we consider a large enough slab, where the wall effects are negligible.

In order to compare results for a uniform field with those of a nonuniform field we plot in the latter case the polarization as a function the average field

$$\bar{E} = \frac{1}{D}\int_0^D E(z)dz. \tag{10}$$

The solid curve in Fig. 8 shows that the polarization for the averaged nonuniform field is similar to that of the uniform field up to $\bar{E} \approx 1$. This value corresponds to $E_0 \approx 2.5$ which in Fig. 4 is where the fluid density near the wall starts to increase. For $\bar{E} \gtrsim 1$ the polarization rapidly increases as the fluid condensates until it saturates at large fields. Hence, the field induced condensation can be utilized to amplify the electric response of a dilute dipolar system that will otherwise follow the Langevin type response.

IV. CONCLUSIONS

We studied the effect of a nonuniform field on a Stockmayer fluid via molecular dynamics simulations. We find that a homogeneous vapor phase in the canonical ensemble, unperturbed by a uniform field, undergoes a significant structural change in a nonuniform field of the same magnitude. This results in a sharp interface separating a liquid like region in the strong field region and a dilute vapor where the field is weaker. We attribute this change to the nonuniform field pulling the dipoles towards the strong field region combined with the attractive short range part of the potential.

Our results indicate that a nonuniform field can be used to quite sensitively control the density profile and hence the fluid properties also in small closed systems. The mechanism we describe should be applicable for a broad class of one-component systems, including molecular fluids and colloidal suspensions. In fact, a nonuniform field should promote phase separation in any dipolar system with an inherent bistable nature [5,6,12,13]. We therefore believe that the study of fluids in nonuniform fields merits further experimental and theoretical attention.

ACKNOWLEDGMENTS

We gratefully acknowledge numerous discussions with A. Arnold and O. Lenz. The work has been performed under the HPC-EUROPA2 project (project no. 228398) with the support of the European Commission - Capacities Area - Research Infrastructures. This work was supported by the Israel Science Foundation under Grant No. 11/10, the COST European program MP1106 "Smart and green interfaces - from single bubbles and drops to industrial, environmental and biomedical applications", and the European Research Council "Starting Grant" No. 259205.

[1] S. H. L. Klapp, J. Phys.: Condens. Matter **17**, R525 (2005).
[2] C. Holm and J.-J. Weis, Curr. Opin. Colloid Interface Sci. **10**, 133 (2005).
[3] Y. Tsori, F. Tournilhac, and L. Leibler, Nature **430**, 544 (2004).
[4] S. Samin and Y. Tsori, J. Phys. Chem. B **115**, 75 (2011).
[5] G. Marcus, S. Samin, and Y. Tsori, J. Chem. Phys. **129**, 061101 (2008).
[6] S. Samin and Y. Tsori, J. Chem. Phys. **131**, 194102 (2009).
[7] M. T. Sullivan, K. Zhao, A. D. Hollingsworth, R. H. Austin, W. B. Russel, and P. M. Chaikin, Phys. Rev. Lett. **96**, 015703 (2006).
[8] M. E. Leunissen, M. T. Sullivan, P. M. Chaikin, and A. van Blaaderen, J. Chem. Phys. **128**, 164508 (2008).
[9] S. O. Lumsdon, E. W. Kaler, and O. D. Velev, Langmuir **20**, 2108 (2004).
[10] D. Bratko, C. D. Daub, K. Leung, and A. Luzar, J. Am. Chem. Soc. **129**, 2504 (2007).
[11] D. Bratko, C. D. Daub, and A. Luzar, PhysChemChemPhys **10**, 6807 (2008).
[12] C. Brunet, J. G. Malherbe, and S. Amokrane, J. Chem. Phys. **131**, 221103 (2009).
[13] C. Brunet, J. G. Malherbe, and S. Amokrane, Phys. Rev. E **82**, 021504 (2010).
[14] A. Z. Panagiotopoulos, Mol. Phys. **61**, 813 (1987).
[15] D. Frenkel and B. Smit, *Understanding Molecular Simulation*, 2nd ed. (Academic Press, San Diego, 2002).
[16] S. Duane, A. Kennedy, B. J. Pendleton, and D. Roweth, Phys. Lett. B **195**, 216 (1987).
[17] B. Mehlig, D. W. Heermann, and B. M. Forrest, Phys. Rev. B **45**, 679 (1992).
[18] H.-J. Limbach, A. Arnold, B. A. Mann, and C. Holm, Comput. Phys. Commun. **174**, 704 (2006).
[19] C. Desgranges and J. Delhommelle, J. Chem. Phys. **130**, 244109 (2009).
[20] J. J. Cerda, V. Ballenegger, O. Lenz, and C. Holm, J. Chem. Phys. **129**, 234104 (2008).
[21] A. Brodka, Chem. Phys. Lett. **400**, 62 (2004).
[22] M. Van Leeuwen, B. Smit, and E. Hendriks, Mol. Phys. **78**, 271 (1993).
[23] K. Kiyohara, K. E. Gubbins, and A. Z. Panagiotopoulos, J. Chem. Phys. **106**, 3338 (1997).
[24] M. J. Stevens and G. S. Grest, Phys. Rev. E **51**, 5976 (1995).
[25] B. Groh and S. Dietrich, Phys. Rev. E **53**, 2509 (1996).
[26] D. Boda, J. Winkelmann, J. Liszi, and I. Szalai, Mol. Phys. **87**, 601 (1996).
[27] K. Kiyohara, K. J. Oh, X. C. Zeng, and K. Ohta, Mol. Simul. **23**, 95 (1999).

[28] I. Szalai, K.-Y. Chan, and Y. W. Tang, Mol. Phys. **101**, 1819 (2003).
[29] R. Jia and R. Hentschke, Phys. Rev. E **80**, 051502 (2009).
[30] L. D. Landau and E. M. Lifshitz, *Elektrodinamika Sploshnykh Sred* (Nauka, Moscow, 1957), Chap. II, Sec. 18, Problem 1.
[31] M. van Leeuwen, Fluid Phase Equilib. **99**, 1 (1994).
[32] J. Bartke and R. Hentschke, Phys. Rev. E **75**, 061503 (2007).
[33] J. Richardi, M. P. Pileni, and J.-J. Weis, Phys. Rev. E **77**, 061510 (2008).
[34] Y. Tsori, Rev. Mod. Phys. **81**, 1471 (2009).
[35] S. H. Lee, J. C. Rasaiah, and J. B. Hubbard, J. Chem. Phys. **85**, 5232 (1986).
[36] P. Debye, *Polar Molecules* (Dover, New York, 1928).
[37] J. Bartke and R. Hentschke, Mol. Phys. **104**, 3057 (2006).
[38] B. Groh and S. Dietrich, Phys. Rev. Lett. **79**, 749 (1997).